Groundwater level spatial variability distribution and risk assessment in a sparsely gauged basin using the Spartan covariance function and auxiliary information

Emmanouil A. Varouchakis[1,2], Kostantinos Kolosionis[1], George. P. Karatzas[1] and Dionissios T. Hristopulos[2]

[1] *School of Environmental Engineering, Technical University of Crete, Chania, Greece, varuhaki@mred.tuc.gr, karatzas@mred.tuc.gr, kkolosionis@gmail.com.*
[2] *School of Mineral Resources Engineering, Technical University of Crete, Chania, Greece, dionisi@mred.tuc.gr.*

Abstract

Knowledge of the spatial variability of the water table level in aquifers that are scarcely monitored provides information to understand the aquifer behaviour at different locations of the basin. This information becomes more important in basins that are under the threat of over-pumping where the water table level has fallen significantly. The spatial distribution feedback gives the potential to identify vulnerable locations. The spatial variability of the water table level in this work is based on hydraulic heads measured during the wet period of the hydrological year 2007-2008, in Mires basin of the Messara valley in Crete, Greece. Three different approaches are used to estimate the spatial variability of the water table level in the basin. All of them are based on Kriging methodology. The first is the classical Ordinary Kriging approach, the second involves information from a secondary variable in terms of Residual Kriging and the third calculates the probability to lie below a certain groundwater level limit that could cause significant problems in groundwater resources availability. The latter is achieved by means of Indicator Kriging. A recently developed non-linear normalization method is used to transform both data and residuals closer to normal distribution for improved prediction results. In addition the recently developed Spartan variogram model is applied to determine the spatial dependence of the measurements. The latter proves to be the optimal model, compared to a series of models tested, that provide in combination with the Kriging methodologies the most accurate cross validation estimations. Groundwater level and probability maps are developed providing the opportunity to assess the spatial variability of the groundwater level in the basin and the risk that certain locations have in terms of a safe groundwater level limit that has been set for the sustainability of the groundwater resources of the basin.

Keywords: Messara valley, groundwater, interpolation, Indicator Kriging, risk assessment, Spartan variogram

Introduction

The accurate mapping of groundwater levels in an aquifer is important for effective management and monitoring decisions. However, the number and spatial distribution of hydraulic head measurements are not always sufficient to accurately represent the groundwater level in a given aquifer. Estimates at unsampled locations can be obtained by applying geostatistical methods to the available data in order to reliably map the free surface of the aquifer. In sparsely monitored basins, accurate mapping of the spatial variability of groundwater level requires the interpolation of scattered data. This work presents the application of Ordinary Kriging, Residual Kriging, and Indicator Kriging to predict the groundwater level spatial variability as well as the associated risk considering the set aquifer level limit (25 meters above sea level) respectively in a sparsely gauged basin.

Ordinary Kriging (OK) bases its estimates at unsampled locations only on the sampled primary variable. OK interpolation is widely used to determine the spatial variability of groundwater levels in hydrological basins e.g., (Theodossiou and Latinopoulos 2006; Ahmadi and Sedghamiz 2007; Nikroo et al. 2009; Sun et al. 2009; Varouchakis and Hristopulos 2013a). Alternatively, Residual Kriging (RK) and Kriging with External Drift (KED), embody secondary information in a drift term. KED and RK are practically equivalent but differ in the methodological steps used (Hengl et al. 2003; Hengl 2007). RK has been applied to the interpolation of water table elevation using deterministic trend models that include e.g.: a) space polynomials (Neuman and Jacobson 1984) b) the topographic elevation and the topographic index (Desbarats et al. 2002; Varouchakis and Hristopulos 2013b), c) numerical solutions for the hydraulic head field (Rivest et al. 2008) and d) rainfall data (Moukana and Koike 2008).

Indicator Kriging (IK) has been widely used for the risk assessment of pollutants concentrations in ground and surface waters that led to significant decisions regarding the prevention and/or remediation of certain sites (Liu et al. 2004; Arslan 2012; Anane et al. 2014). However, it can be also applied for the risk assessment of groundwater level spatial distribution in arid areas or in those with high aquifer pumping.

Area of Study

The present research focuses on Mires basin of the Messara Valley (Fig. 1) at the island of Crete (Greece). The study area is a sparsely sampled basin that has limited groundwater resources which are vital for the area’s ecosystem and agriculture. Knowledge of the spatial variations of groundwater level is important for developing sound management and monitoring strategies. Over-exploitation during the past 30 years has led to a dramatic decrease, in excess of 35 m, of the groundwater level. Efficient groundwater management in the basin is crucial in light of predictions based on regional climate change models that show a substantial risk of desertification for Crete. In this work accurate spatial models of the basin’s groundwater level are generated that help to identify the susceptible locations and to provide input for potential groundwater resources management plans. The data used in this research consist of 42 hydraulic head measurements (wet period of 2007-2008 hydrological year) from the 70 monitoring locations that operate in the basin which are unevenly distributed and mostly concentrated along a temporary river. The range of hydraulic heads varies from an extremely low value of 11.45 meters above sea level (masl) to 72.93 masl. An initial statistical analysis shows that the head data have skewness and kurtosis coefficients equal to $\hat{s}_z = 0.76$ and $\hat{k}_z = 2.80$ respectively, implying a mild deviation from Gaussian statistics ($\hat{s}_z = 0$ and $\hat{k}_z = 3$ respectively).

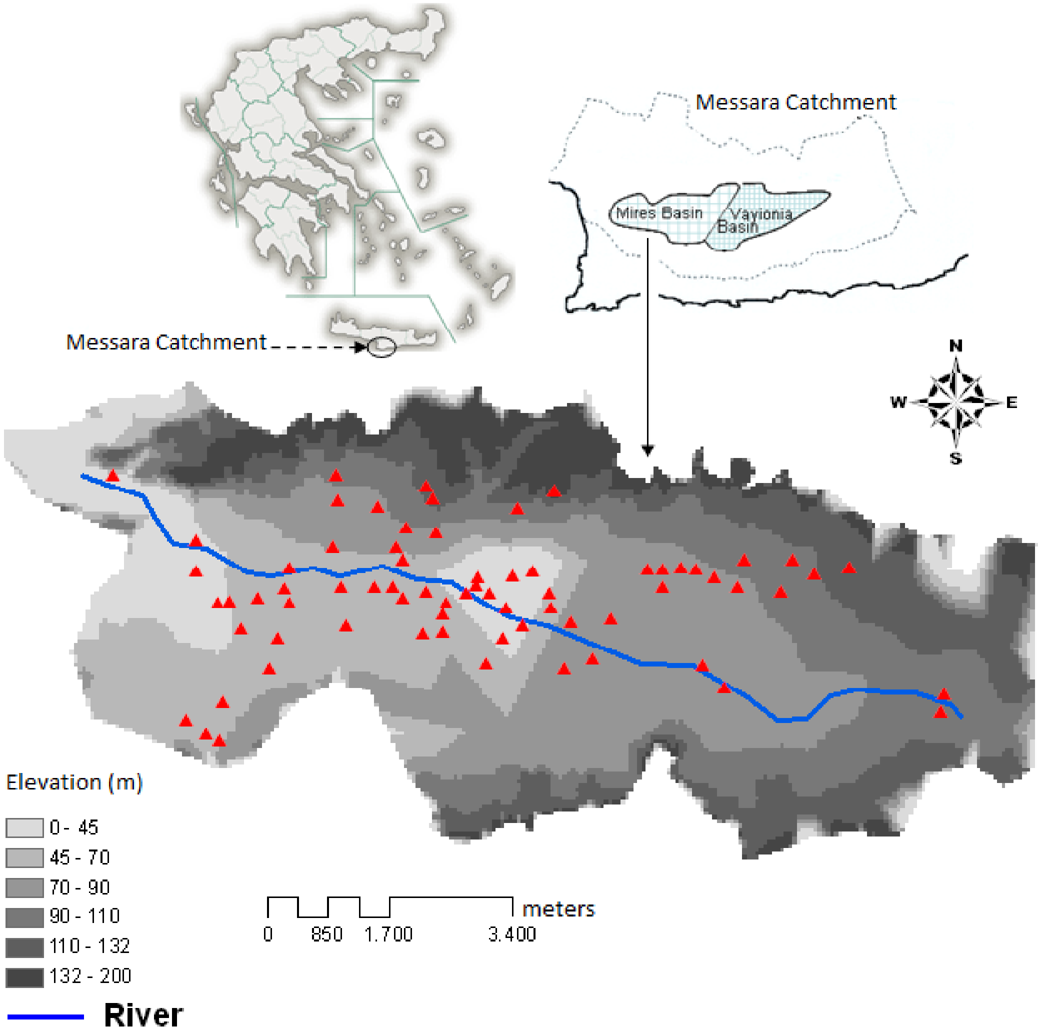

Figure 1. Map of Greece showing the Messara Catchment (black ellipse) in Crete and the Mires basin locations accompanied by a topographic map showing the locations of groundwater head measurement in Mires basin along with the corresponding surface elevation and the temporary river path.

Methodology

Skewed or erratic data can often be made more suitable for geostatistical modeling by appropriate transformation. A normal distribution for the variable under study is desirable in linear geostatistics (Clark and Harper 2000). Even though normality may not be strictly required, serious violation of normality, such as too high skewness and outliers, can impair the variogram structure and the Kriging results (Gringarten and Deutsch 2001; Mcgrath et al. 2004). Ordinary Kriging is well-known to be optimal when the data have a multivariate normal distribution. Transformation of data therefore may be required before Kriging to normalize the data distribution, suppress outliers and improve data stationarity (Deutsch and Journel 1992; Armstrong 1998). The estimation then is performed in the Gaussian domain before back-transforming the estimates to the original domain. An advantage of the Gaussian distribution is that spatial variability is easier to be modelled because it reduces effects of extreme values providing more stable variograms. (Goovaerts 1997; Armstrong 1998; Pardo-Iguzquiza and Dowd 2005). Kriging represents variability only upto the second order moment (covariance), so the random field of the transformed variable must therefore be Gaussian to derived unbiased estimates at non-sampled locations (Deutsch and Journel 1992; Goovaerts et al. 2005).

A non-linear normalizing data transformation is applied in conjunction with Kriging for the accurate prediction of groundwater level spatial variability. The Modified Box-Cox (MBC) transformation method has recently been proposed and applied successfully to normalize hydraulic heads and residuals (Varouchakis et al. 2012). Besides the classical OK interpolation, the prediction of the hydraulic head spatial variability is also performed using RK by incorporating local geographic features, such as the ground surface elevation in the trend function. Previous studies have shown that incorporating such auxiliary information in the trend function improves the accuracy of the spatial interpolation (Varouchakis 2012). Evaluation of the performance and interpolation errors of OK and RK in the estimation of water level elevation can be achieved by means of leave-one-out cross validation.

In the following, it is assumed that the hydraulic head is represented by a spatial random field (SRF), which herein will be in generally denoted by $Z(\mathbf{s},\omega)$, where ω is the state index used to denote that $Z(\mathbf{s},\omega)$ is a realization from an ensemble of possible states (to be omitted for brevity). The sampled field at the measurement points will be denoted by $Z(\mathbf{s}\in S)$, where S is the set of sampling points with cardinal number N. The values of the SRF in a given state will be denoted by lower-case letters. The target is to derive estimates, $\hat{Z}(\mathbf{s}\in P)$ of the head at the prediction set points, P that lie on a rectangular grid that covers the basin. Therefore, $\mathbf{s}_i, i=1,\ldots,N$ denote the sampling points, $z(\mathbf{s}_i)$ are the head values (in masl) at these points, and $\mathbf{s}_0$ denotes an estimation point, which is assumed to lie inside the convex hull of the sampling network. For mapping purposes, it is assumed that $\mathbf{s}_0$ moves sequentially through all the nodes of the mapping grid.

Herein the interpolation estimates are kept within the convex hull of the sampling points. In principle maps can be estimated over the entire study domain; however, this is equivalent to extrapolation. Kriging can be used for extrapolation but the results outside the quadrilateral, determined from the sampling locations boundaries, are often less accurate and subject to higher uncertainty. In addition the variogram is determined by the measurements and expresses the spatial dependence of the measured points. In performing extrapolation, it is accepted that the variogram is valid outside the range of measurements. Therefore the estimates inside the quadrilateral are more accurate and precise than those outside.

For spatial interpolation initially OK method is applied and then RK in combination with MBC normalizing transformation. In the first approach, a normalizing transformation $g(\cdot)$ is applied to the data. Then, OK is used to predict the transformed field $Y(\mathbf{s})=g\left(Z(\mathbf{s})\right)$, and the predictions are back-transformed to obtain head estimates. In the second approach, a trend model $m_Z(\mathbf{s})$ is introduced that captures local features. Since the fluctuation SRF, $Z'(\mathbf{s})=Z(\mathbf{s})-m_Z(\mathbf{s})$, is non-Gaussian, a transformation $g(\cdot)$ is applied to obtain a normalized SRF, $Y(\mathbf{s})=g\left(Z'(\mathbf{s})\right)$, the experimental variogram is then estimated and is fitted to theoretical models. Next, the Gaussian field $\hat{Y}(\mathbf{s}\in P)$ is estimated at the prediction points using OK. Finally, head estimates are retrieved from $\hat{Y}(\mathbf{s}\in P)$ by applying the back-transformation and adding the trend. Leave-one-out cross-validation analysis is used to determine the optimal spatial model and to assess the accuracy of the interpolated head field.

Spatial models

Linear interpolation methods such as OK and RK are examined for mapping spatial groundwater level variability. In spatial linear interpolation methods, it generally holds that,

$$\hat{z}(\mathbf{s}_0) = \sum_{\{i:\mathbf{s}_i \in S_0\}} \lambda_i \, z(\mathbf{s}_i) \,, \quad (1)$$

where S_0 is the set of sampling points in the search neighborhood of $\mathbf{s}_0$. The neighborhood is empirically chosen so as to optimize the cross validation measures. The weights λ_i are obtained by minimizing the mean square estimation error conditionally on the zero-bias constraint (Cressie 1993), and they depend on the variogram model $\gamma_z(\mathbf{r})$ (Deutsch and Journel 1992). The OK estimation variance is given by the following equation, with the Lagrange coefficient μ compensating for the uncertainty of the mean value:

$$\sigma_E^2(\mathbf{s}_0) = \sum_{\{i:\mathbf{s}_i \in S_0\}} \lambda_i \, \gamma_z(\mathbf{s}_i, \mathbf{s}_0) + \mu \,. \quad (2)$$

Overall OK variance is termed as the weighted average of variograms from the new point $\mathbf{s}_0$ to all calibration points $\mathbf{s}_j$, plus the Lagrange multiplier.

RK combines a trend function with interpolation of the residuals. In RK the estimate is expressed as:

$$\hat{z}(\mathbf{s}_0) = m_z(\mathbf{s}_0) + \hat{z}'(\mathbf{s}_0) \,, \quad (3)$$

where $m_z(\mathbf{s}_0)$ is the trend function, and $\hat{z}'(\mathbf{s}_0)$ is the interpolated residual by means of OK (Rivoirard 2002). Typically, the trend function is modeled as:

$$m_z(\mathbf{s}_0) = \sum_{k=0}^{p} \beta_k \, q_k(\mathbf{s}_0) \,; \; q_k(\mathbf{s}_0) \equiv 1 \,, \quad (4)$$

where $q_k(\mathbf{s}_0)$ are the values of auxiliary variables at $\mathbf{s}_0$, β_k are the estimated regression coefficients and *p* is the number of auxiliary variables (Draper and Smith 1981; Hengl 2007; Hengl et al. 2007). Auxiliary variables could include polynomials of the data coordinates (x,y). The regression coefficients are estimated from the sample using ordinary least squares (OLS) (Kitanidis 1993). The variance of the estimates follows from the equation (Hengl et al. 2003; Hengl 2007):

$$\sigma^2(\mathbf{s}_0) = \sigma_d^2(\mathbf{s}_0) + \sigma_f^2(\mathbf{s}_0) \,, \quad (5)$$

where $\sigma_d^2(\mathbf{s}_0)$ is the drift prediction variance, and $\sigma_f^2(\mathbf{s}_0)$ is the Kriging (OK) variance of residuals.

Modified Box-Cox (MBC)

This new method focuses on normalizing the skewness and kurtosis coefficients of the data, but it neglects higher-order moments (Varouchakis and Hristopulos 2013b). It is defined by the following function,

$$y := g_{MBC}(z;\boldsymbol{\kappa}) = \frac{\left(z - z_{\min} + k_2{}^2\right)^{k_1} - 1}{k_1}, \; \boldsymbol{\kappa}^T = (k_1, k_2), \quad (6)$$

where k_1 is the power exponent and k_2 is an offset parameter. Use of the latter allows negative *z* values and so the transformation can be applied to fluctuations as well. Parameters (k_1, k_2) are estimated from the numerical solution of the equations $\hat{s}_z = 0, \hat{k}_z = 3$, where $\hat{s}_z$ and $\hat{k}_z$ are the sample skewness and kurtosis coefficients respectively,

$$\left(\frac{\hat{m}_z - \tilde{m}_z}{\sigma_z}\right)^2 + \left(\hat{k}_z - 3\right)^2 \to 0, \quad (7)$$

where $\hat{m}_z$ is the sample mean, $\tilde{m}_z$ is the sample's median and σ_z the standard deviation. The minimization is performed using the Nelder-Mead simplex optimization method (Nelder and Mead 1965; Press et al. 1992). The application of the methodology to the initial head dataset improves their normality (Tab. 1).

Table 1. Normalization results using Modified Box-Cox (MBC) transformation: skewness coefficient $\hat{s}_z$; kurtosis coefficient $\hat{k}_z$.

	$\hat{s}_z$	$\hat{k}_z$
Initial head data	0.76	2.80
MBC	-0.15	2.99

Spatial dependence

The variogram is commonly used in geostatistical analysis to measure the spatial dependence between neighboring observations. The omnidirectional empirical (experimental) variogram of the hydraulic head and of the residuals is determined using the method of moments. The empirical variogram is fitted with isotropic classical models, the Matérn model (Goovaerts 1997), and the new family of Spartan variograms (Hristopulos 2003; Hristopulos and Elogne 2007).

Spartan Spatial Random Fields (SSRFs) are a geostatistical model (Hristopulos 2002; Hristopulos 2003) inspired from statistical field theory with applications in environmental risk assessment and environmental monitoring (Elogne et al. 2008; Elogne and Hristopulos 2008; Hristopulos and Elogne 2009). SSRFs are generalized Gibbs random fields with an energy functional that is based on local interactions between the field values. The term Spartan indicates parametrically compact model families that involve a small number of parameters. SSRFs provide a new class of generalized covariance functions. The SSRFs covariance functions can be used for spatial interpolation with the classical Kriging estimators. Spartan covariance and variogram functions have been applied to various environmental data sets (Elogne et al. 2008, Varouchakis and Hristopulos 2013b). Herein, the Spartan covariance derived for d = 3 dimensions is applied. The Spartan parameters can be estimated by fitting the SSRFs variogram to the empirical variogram estimator. The Spartan covariance functions in d = 3 dimensions are expressed as follows (Hristopulos and Elogne 2007):

$$C_z(\mathbf{h}) = \begin{cases} \dfrac{\eta_0\, e^{-h\beta_2}}{2\pi\sqrt{|\eta_1^2-4|}}\left[\dfrac{\sin(h\beta_1)}{h\beta_1}\right], & \text{for } |\eta_1|<2,\ \sigma_z^2 = \dfrac{\eta_0}{2\pi\sqrt{|\eta_1^2-4|}} \\ \dfrac{\eta_0\, e^{-h}}{8\pi}, & \text{for } \eta_1 = 2,\ \sigma_z^2 = \dfrac{\eta_0}{8\pi} \\ \dfrac{\eta_0\,(e^{-h\omega_1}-e^{-h\omega_2})}{4\pi(\omega_2-\omega_1)\,h\sqrt{|\eta_1^2-4|}}, & \text{for } \eta_1 > 2,\ \sigma_z^2 = \dfrac{\eta_0}{4\pi\sqrt{|\eta_1^2-4|}} \end{cases} . \quad (8)$$

In the above, η_0 is the scale factor, η_1 is the rigidity coefficient, $\beta_1 = |2-\eta_1|^{1/2}/2$ is a dimensionless wavenumber, $\beta_2 = |2+\eta_1|^{1/2}/2$ and $\omega_{1,2} = \left(|\eta_1 \mp \Delta|/2\right)^{1/2}$, $\Delta = |\eta_1^2-4|^{1/2}$, are dimensionless damping coefficients, ξ is a characteristic length, $\mathbf{h} = \mathbf{r}/\xi$ is the normalized lag vector, $h = |\mathbf{h}|$ is its Euclidean norm and σ_z^2 is the variance. A covariance function that is permissible in three spatial dimensions is also permissible in two dimensions (Christakos 1991). Hence, it can be used in two dimensions. The exponential covariance is recovered for η_1 = 2, while for $|\eta_1|$ < 2 the product of the exponential and hole-effect model is obtained.

Trend Modeling of Hydraulic Head in Mires Basin

Below a trend model for Mires basin is presented. Following other studies, secondary information in the trend is considered from a Digital Elevation Model (DEM) of the area (Hoeksema et al. 1989; Deutsch and Journel 1992; Goovaerts 1997; Desbarats et al. 2002; Rivest et al. 2008; Nikroo et al. 2009). The correlation coefficient of the groundwater level and the ground surface elevation in Mires basin is calculated at 0.65, a value that is characterized as important (Tichy 1993). The following expression for the trend of the hydraulic head (in masl) is proposed (T-DEM):

$$m_z(\mathbf{s}) = f\, DEM(\mathbf{s}) + c\,, \quad (9)$$

where f, c are linear coefficients and $DEM(\mathbf{s})$ is the local DEM value. The residuals of the trend model also display deviations from normality that are reduced by means of the MBC transformation (Tab. 2).

Table 2. Skewness $\hat{s}_z$ and kurtosis $\hat{k}_z$ coefficients of trend models residuals following modified Box-Cox (MBC) normalization

	$\hat{s}_z$	$\hat{k}_z$
Residuals	0.35	2.5
MBC	-0.10	3.0

Indicator Kriging

IK (Goovaerts 1997) is a non-parametric geostatistical method for estimating the probability of a variable to exceed or lie below a specific threshold value at a given location. In this work, IK is applied for mapping the risk associated with a specified groundwater level limit that could lead to significant problem of groundwater availability. IK is applied to determine the conditional probability at unsampled points based on the spatial dependence structure of indicator-transformed data points with a binary distribution (e.g. 0 and 1). IK proceeds as the classical Ordinary Kriging (the main change is the choice of a cutoff value) with the difference that results is now maps with values between 0 and 1 expressing probability a condition to apply. Indicator variogram analysis is also performed using the models and the procedure previously stated for OK and RK (Isaaks and Srivastava 1989).

This method does make assumptions regarding the variables distribution and has the ability to take into account, to a large extent, the uncertainty of the data. The IK is based on the conversion of all of our data from continuous to a binary form according to a specific threshold value. This value can be either a percentile of our data or default value of marginal importance for the system under study. Subsequently, data with values below the threshold take a value of 1, while the remaining taking a value of 0.

$$I\left(z(\mathbf{s})\right) = \begin{cases} 1, & z(\mathbf{s}) \le z' \\ 0, & otherwise \end{cases}, \quad (10)$$

where, $I\left(z(\mathbf{s})\right)$ is a binary variable, $z(\mathbf{s})$ is the measured value and z' is the cut-off (threshold) value.

Indicator Kriging is a geostatistical method best suited for issues that involve a threshold value (Isaaks and Srivastava 1989; Goovaerts 1999; Webster and Oliver 2001). However, most practical problems that require indicator techniques require well-chosen threshold which have a special significance to the problem being addressed. Probability maps delineate suitable and unsuitable sites regarding the examined issue while, help to take decisions to prevent and/or remediate a site compared to locations with reduced or no risk.

The method proceeds as follows: a) convert the given values to indicators: divide the range evenly or based on different quintiles ($q_{0.25}$; $q_{0.50}$; $q_{0.75}$), b) estimate the indicator variogram, c) apply Kriging using the usual equations and obtain predictions. On the other hand the methodology has a set of disadvantages such as it will not necessarily provide probabilities to add up to 1 and sometimes the prediction may end up beyond interval [0, 1] (e.g. Kriging occasionally provides negative weights-screening effect).

Results and Discussion

The performance of the Kriging-based geostatistical models is evaluated by using the leave one out cross validation technique that is usually applied in small datasets (Witten et al. 2011). A series of well known statistical measures is employed to compare the true and estimated values of the cross-validation procedure, such as the correlation coefficient R, the Mean Absolute Error (MAE), the Root Mean Square Error (RMSE) and the Mean Absolute Relative Error (MARE).

The general approach that is used for interpolation applies a normalizing transformation followed by OK on the transformed variable, and it finally back-transforms the predictions. In terms of the spatial model that considers the head data the parameters of the theoretical variogram models tested (Gaussian, Exponential, Linear, Spartan, Matérn, Spherical, and Power-law) are obtained by least squares fitting to the experimental omnidirectional variogram of the transformed hydraulic head. The Spartan model gives the best fit in terms of cross validation results (Tab. 3) while the Spherical and the Matérn variogram come close.

Table 3. Cross validation measures for spatial MBC-OK model with optimal variograms: MBC & OK: Ordinary Kriging with modified Box-Cox transformation of data and back-transformation. SP: Spartan variogram. SPH: Spherical variogram. M: Matérn variogram.

Method	**Variogram model**	**MAE** (masl)	**BIAS** (masl)	**MARE**	**RMSE** (masl)	**R**
MBC & OK	SP	5.32	0.03	0.17	7.20	0.90
	SPH	5.41	0.08	0.17	7.43	0.90
	M	5.65	0.04	0.18	7.70	0.89

In the case of spatial model with trend component RK is applied. RK combines a trend function with interpolation of the residuals. The omnidirectional experimental variogram is calculated by applying the method of moments to the transformed residuals of the T-DEM model. The MBC transformation is used to normalize the residuals (Tab. 2). The Spartan variogram model (Fig. 2) again provides the best fit in terms of cross validation results (Tab. 4). The Spherical variogram provides similar results to the Spartan model while third best is the Matérn model.

Table 4. Cross validation measures for spatial MBC-RK-T-DEM model with optimal variograms: trend using DEM surface elevation. MBC & RK: Residual Kriging with modified Box-Cox transformation of residuals and back-transformation. SP: Spartan variogram. SPH: Spherical variogram. M: Matérn variogram.

Method	**Variogram model**	**MAE** (masl)	**BIAS** (masl)	**MARE**	**RMSE** (masl)	**R**
MBC & RK	SP	4.27	0.07	0.15	5.90	0.91
	SPH	4.46	0.05	0.15	6.23	0.90
	M	4.75	0.08	0.16	6.50	0.88

The MBC-RK approach improves significantly the mean absolute prediction error (4.27 masl) by over 1 m compared to the MBC-OK (5.32 masl) approach. In addition the other estimation measures are at least similar (BIAS) but mostly improved (RMSE, R, MARE). Considering overall the cross validation measures the estimates based on the Spartan model prevails compared to the other two optimal models.

The least squares sum for each fitted variogram model is considered, which is an index of optimal fitting, for selecting the optimal variogram model with Indicator Kriging interpolation. Spartan model achieves the best fit (Fig. 3) over the range of lags considered providing a value of 0.023 compared to 0.029 for the spherical and 0.031 for the Matérn models.

The T-DEM trend model with RK and the IK methodology are applied to estimate the groundwater level and the probabilities of groundwater level to lie below a threshold value on a 100 x 100 grid defined in normalized coordinate space (actual cell size: 114 x 47 m). In addition the uncertainties of the estimations are also determined on a same grid size. Estimates are obtained only at points that lie inside the convex hull of the measurement locations (7317 grid points). The contour maps in physical space are shown in figures 4 to 7. The residuals of the T-DEM model are interpolated using the Spartan variogram model (Fig. 2) with the following optimal parameter values: σ^2 = 17.77, ξ = 0.27 (in normalized units), $\eta_1 =$ -1.99 while the indicators applying the Spartan variogram model (Fig. 3) with optimal parameter values: σ^2 = 0.25, ξ = 0.26 (in normalized units), $\eta_1 =$ -1.90. The optimum search radius used with the Spartan model (determined by the leave-one-out cross validation test) is equal to 0.38 (normalized units) for both models. Near the origin and at intermediate distances, which are crucial for the interpolation, the Spartan model fitting is very good and overall follows the trend of the experimental variogram. The negative values of η_1 causes a negative hole effect in the Spartan correlation (Žukovič and Hristopulos 2008) that can be observed in both variogram figures (Fig. 2 and Fig. 3).

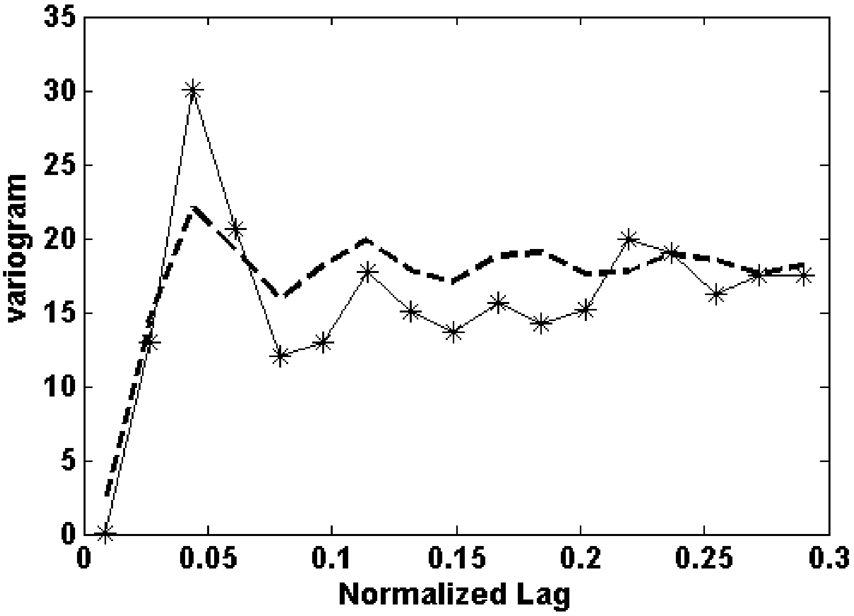

Figure 2. Plot of omnidirectional variogram of residuals (stars) after applying MBC normalization and the best-fit Spartan variogram (SP) model fit (dashed line). The residuals are derived by applying to the trend the ground surface elevation (T-DEM)

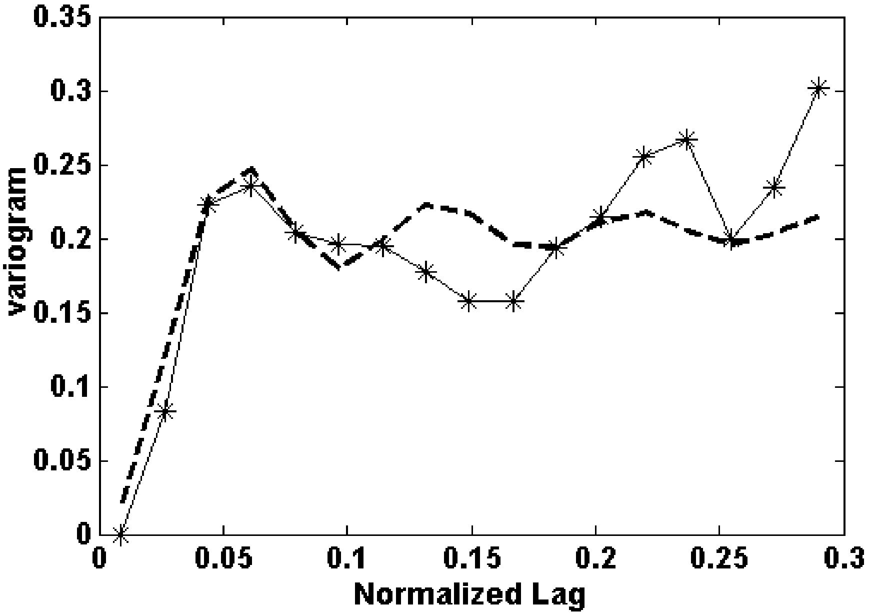

Figure 3. Indicator omnidirectional variogram and the best-fit Spartan semivariogram (SP) model fit (dashed line).

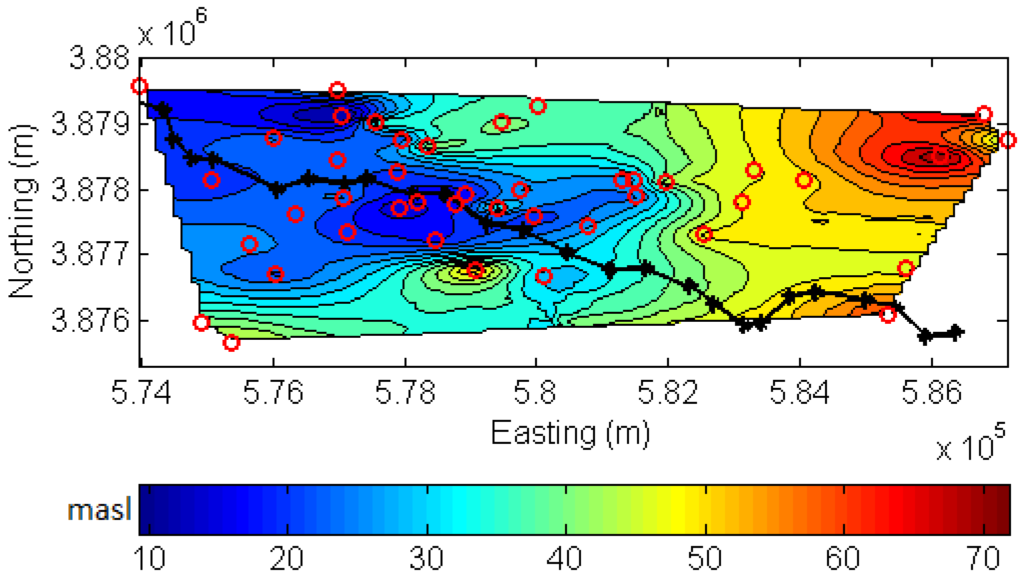

Figure 4. Map of estimated groundwater level in the Mires basin using MBC-RK-T-DEM spatial model, adapted on the real basin coordinates and location in the valley (circles denote the monitoring locations and solid black line the temporary river path).

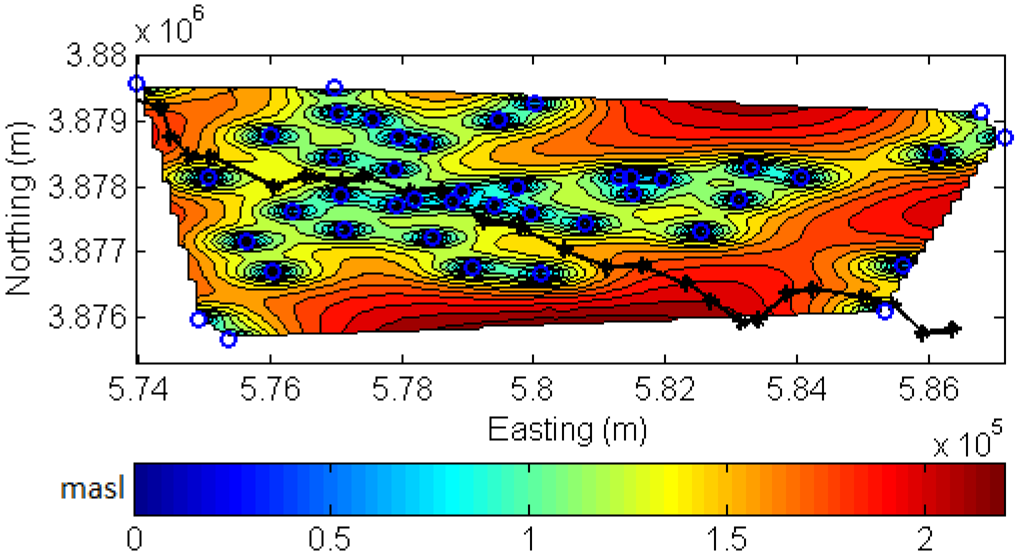

Figure 5. Map of estimated groundwater level standard deviation in the Mires basin using MBC-RK-T-DEM spatial model, adapted on the real basin coordinates and location in the valley (circles denote the monitoring locations and solid black line the temporary river path).

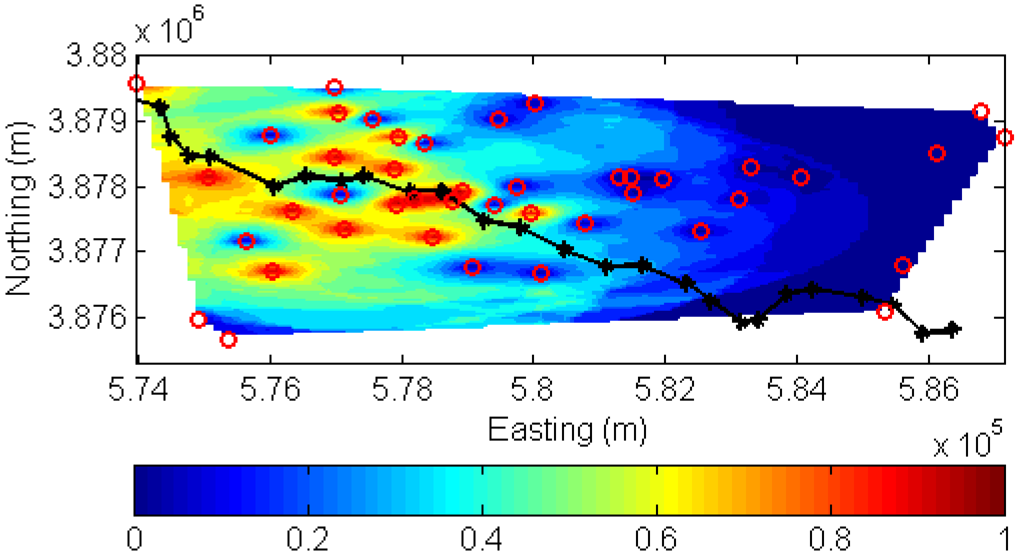

Figure 6. Map of estimated probabilities in the Mires basin using IK, adapted on the real basin coordinates and location in the valley (circles denote the monitoring locations and solid black line the temporary river path).

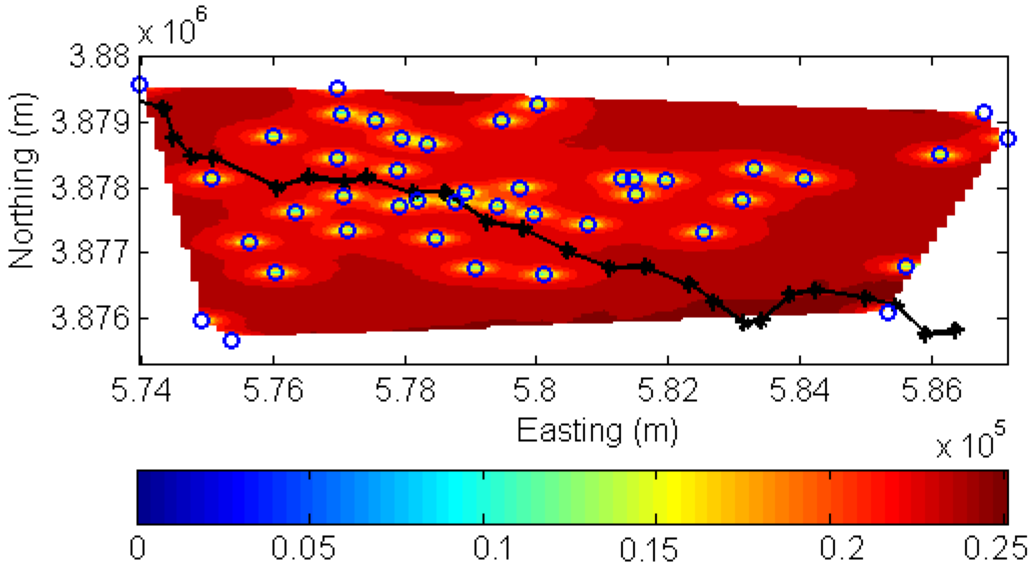

Figure 7. Map of estimated probabilities standard deviation in the Mires basin using IK, adapted on the real basin coordinates and location in the valley (circles denote the monitoring locations and solid black line the temporary river path).

The groundwater level map of the basin (Fig. 4) presents the spatial variability of the groundwater level that changes from East towards West direction following the ground surface elevation trend (Fig. 1). The higher levels are met at the East of the basin while the lowest towards the West. The error map (Fig. 5) identifies the locations of the Mires Basin with the largest Kriging standard deviation. Hence, the borders of the basin can benefit from further sampling according to RK standard deviation results. Indicator Kriging predictions (Fig. 6) shows that in the center and towards the West borders of the basin the risk of the aquifer level to decline below the set 25 m threshold is significant. Probabilities are increased closer to the river path than higher away. The dependence is reasonable considering that the agricultural activity in the area is concentrated along the temporary river.

Conclusions

The optimal spatial interpolation approach for the spatial variability of the groundwater level in Mires basin is based on Residual Kriging with the Spartan variogram model applied to the normalized (MBC) fluctuations. The present findings are supported by the results of cross validation analysis. In addition, risk maps based on IK identify the vulnerable areas of the basin that require intense monitoring and remedial actions to avoid further decline of the aquifer. These are located at the west part of the basin mainly along the river path. The newly developed MBC transformation method shows an excellent behaviour transforming both data and residuals closer to normal distribution. In addition the Spartan variogram model has an excellent fit to the experimental variogram of the data, residuals and indicators following closely their trend. Thus, it constitutes a reliable alternative to assess the spatial dependence of groundwater level data in interpolation studies.

References

Ahmadi S. and Sedghamiz A., 2007. Geostatistical analysis of spatial and temporal variations of groundwater Level. Environmental Monitoring and Assessment, 129, 277-294.

Anane M., Selmi Y., Limam A., Jedidi N. and Jellali S., 2014. Does irrigation with reclaimed water significantly pollute shallow aquifer with nitrate and salinity? An assay in a perurban area in North Tunisia. Environmental Monitoring and Assessment, 186, 4367-4390.

Armstrong M., 1998. Basic linear geostatistics. Springer Verlag, Berlin.

Arslan H., 2012. Spatial and temporal mapping of groundwater salinity using ordinary kriging and indicator kriging: The case of Bafra Plain, Turkey. Agricultural Water Management, 113, 57-63.

Christakos G., 1991. Random field models in earth sciences. Academic press, San Diego.

Clark I. and Harper W. V., 2000. Practical Geostatistics 2000. Ecosse North America Llc, Columbus, Ohio, USA.

Cressie N., 1993. Statistics for spatial data (revised ed.). Wiley, New York.

Desbarats A. J., Logan C. E., Hinton M. J. and Sharpe D. R., 2002. On the kriging of water table elevations using collateral information from a digital elevation model. Journal of Hydrology, 255, 25-38.

Deutsch C. V. and Journel A. G., 1992. GSLIB. Geostatistical software library and user's guide. Oxford University Press, New York.

Draper N. and Smith H., 1981. Applied Regression Analysis. Wiley, New York.

Elogne S., Hristopulos D. and Varouchakis E., 2008. An application of Spartan spatial random fields in environmental mapping: focus on automatic mapping capabilities. Stochastic Environmental Research and Risk Assessment, 22, 633-646.

Elogne S. N. and Hristopulos D. T., 2008. Geostatistical applications of Spartan spatial random fields. geoENV VI - Geostatistics for environmental applications in series: Quantitative geology and geostatistics. In: A. Soares, M. J. Pereira and R. Dimitrakopoulos (eds). Berlin, Gemany: Springer, 15, 477-488.

Goovaerts P., 1997. Geostatistics for natural resources evaluation. Oxford University Press, New York.

Goovaerts P., 1999. Geostatistics in soil science: state-of-the-art and perspectives. Geoderma, 89, 1-45.

Goovaerts P., AvRuskin G., Meliker J., Slotnick M., Jacquez G. and Nriagu J., 2005. Geostatistical modeling of the spatial variability of arsenic in groundwater of southeast Michigan. Water Resources Research, 41.

Gringarten E. and Deutsch C. V., 2001. Teacher's aide: Variogram interpretation and modeling. Mathematical Geology, 33, 507–534.

Hengl T., 2007. A practical guide to geostatistical mapping of environmental variables. EUR 22904 EN-Scientific and Technical Research series. Luxembourg: Office for Official Publications of the European Communities, pp. 143,

Hengl T., Geuvelink G. B. M. and Stein A., 2003. Comparison of kriging with external drift and regression-kriging. Technical note, ITC, Available on-line at http://www.itc.nl/library/Academic output/.

Hengl T., Heuvelink G. B. M. and Rossiter D. G., 2007. About regression-kriging: From equations to case studies. Computers & Geosciences, 33, 1301-1315.

Hoeksema R. J., Clapp R. B., Thomas A. L., Hunley A. E., Farrow N. D. and Dearstone K. C., 1989. Cokriging model for estimation of water table elevation. Water Resources Research, 25, 429–438.

Hristopulos D. T., 2002. New anisotropic covariance models and estimation of anisotropic parameters based on the covariance tensor identity. Stochastic Environmental Research and Risk Assessment, 16, 43-62.

Hristopulos D. T., 2003. Spartan Gibbs random field models for geostatistical applications. SIAM Journal on Scientific Computing, 24, 2125-2162.

Hristopulos D. T. and Elogne S. N., 2007. Analytic properties and covariance functions for a new class of generalized Gibbs random fields. IEEE Transactions on Information Theory, 53, 4667-4467.

Hristopulos D. T. and Elogne S. N., 2009. Computationally efficient spatial interpolators based on Spartan spatial random fields. IEEE Transactions on Signal Processing, 57, 3475-3487.

Isaaks E. H. and Srivastava R. M., 1989. An introduction to applied geostatisics. Oxford University Press, New York.

Kitanidis P., 1993. Generalized covariance functions in estimation. Mathematical Geology, 25, 525-540.

Liu C.-W., Jang C.-S. and Liao C.-M., 2004. Evaluation of arsenic contamination potential using indicator kriging in the Yun-Lin aquifer (Taiwan). Science of The Total Environment, 321, 173-188.

Mcgrath D., Zhang J. E. and Qu L. T., 2004. Temporal and spatial distribution of sediment total organic carbon in an estuary river. J Environ Qual, 35, 93–100.

Moukana J. A. and Koike K., 2008. Geostatistical model for correlating declining groundwater levels with changes in land cover detected from analyses of satellite images. Computers & Geosciences, 34, 1527-1540.

Nelder J. A. and Mead R., 1965. A simplex method for function minimization. Computer Journal, 7, 308-313.

Neuman S. and Jacobson E., 1984. Analysis of nonintrinsic spatial variability by residual kriging with application to regional groundwater levels. Mathematical Geology, 16, 499-521.

Nikroo L., Kompani-Zare M., Sepaskhah A. and Fallah Shamsi S., 2009. Groundwater depth and elevation interpolation by kriging methods in Mohr Basin of Fars province in Iran. Environmental Monitoring and Assessment, 166, 387-407.

Pardo-Iguzquiza E. and Dowd P., 2005. Empirical maximum likelihood Kriging: The general case. Mathematical Geology, 37, 477-492.

Press W. H., Teukolsky S. A., Vettering W. T. and Flannery B. P., 1992. Numerical Recipes in Fortran. Cambridge University Press., New York.

Rivest M., Marcotte D. and Pasquier P., 2008. Hydraulic head field estimation using kriging with an external drift: A way to consider conceptual model information. Journal of Hydrology, 361, 349-361.

Rivoirard J., 2002. On the Structural Link Between Variables in Kriging with External Drift. Mathematical Geology, 34, 797-808.

Sun Y., Kang S., Li F. and Zhang L., 2009. Comparison of interpolation methods for depth to groundwater and its temporal and spatial variations in the Minqin oasis of northwest China. Environmental Modelling & Software, 24, 1163-1170.

Theodossiou N. and Latinopoulos P., 2006. Evaluation and optimisation of groundwater observation networks using the kriging methodology. Environmental Modelling & Software, 21, 991-1000.

Tichy M., 1993. Applied methods of structural reliability. Springer, Dordrecht.

Varouchakis E. A., 2012. Geostatistical Analysis and Space-Time Models of Aquifer Levels: Application to Mires Hydrological Basin in the Prefecture of Crete, PhD Thesis, Technical University of Crete, Chania.

Varouchakis E. A. and Hristopulos D. T., 2013a. Comparison of stochastic and deterministic methods for mapping groundwater level spatial variability in sparsely monitored basins. Environmental Monitoring and Assessment, 185, 1-19.

Varouchakis E. A. and Hristopulos D. T., 2013b. Improvement of groundwater level prediction in sparsely gauged basins using physical laws and local geographic features as auxiliary variables. Advances in Water Resources, 52, 34-49.

Varouchakis E. A., Hristopulos D. T. and Karatzas G. P., 2012. Improving kriging of groundwater level data using nonlinear normalizing transformations-a field application. Hydrological Sciences Journal, 57, 1404-1419.

Webster R. and Oliver M., 2001. Geostatistics for environmental scientists: Statistics in practice. Wiley, Chichester.

Witten I. H., Frank E. and Hall M. A., 2011. Data Mining: Practical Machine Learning Tools and Techniques: Practical Machine Learning Tools and Techniques. Elsevier, San Francisco.

Žukovič M. and Hristopulos D. T., 2008. Environmental time series interpolation based on Spartan random processes. Atmospheric Environment, 42, 7669-7678.